CALCULATION OF THE FLOW OF A GAS WITH PARTICLES PAST BLUFF BODIES WITH ALLOWANCE FOR THE EFFECT OF REFLECTED PARTICLES ON THE FLOW OF THE AEROSOL

Yu. M. Davydov, I. Kh. Enikeev,
and R. I. Nigmatulin

UDC 532.529

The boundary conditions on a body in a an aerosol have a significant effect on the hydrodynamics of the gas and particles. a number of theoretical studies of such flows have assumed that particles which fall onto the surface of the body disappear from the flow, i.e., that the surface of the body is a particle sink [1-3]. Such a formulation of the problem is most appropriate when liquid drops or particles which form a thin film on the surface after striking it are regarded as the disperse phase. If the disperse phase consists of solid particles, then the formulation often must be made more complex: it is necessary to introduce an additional phase — a phase consisting of particles reflected from the surface of the body in the flow. Most of the works in which reflected particles have been studied have been experimental investigations [4-7]. The few thoeretical studies have been made with the assumption that the mass concentration of particles is low. This makes it possible to examine the motion of reflected particles within a specified field of gas velocities [8, 9]. Matveev [10] proposed a model which makes it possible to study flow past a body in the presence of a layer of randomly moving particles located near the surface of the body. This particle layer is regarded a s a layer of a second "gas" having a Maxwell distribution of particles (molecules) with respect to velocity. Separate calculations were performed in [11] with allowance for the effect of reflected particles on flow hydrodynamics. Here, no consideration was given to the collisions of incident and reflected particles.

In the present investigation, we propose a mathematical model and method of calculation which permit use of a three-velocity, three-temperature scheme of motion of interpenetrating continua to numerically study a broad range of problems concerning the aerodynamics of disperse flows. We indicate the ranges of the governing parameters within which it is important to allow for the thermal and velocity disequilibria of the phases. The basic similarity criteria for the given class of problems are also formulated.

1. Formulation of the Problem. We will examine the transverse flow of an aerosol past a flat plate with allowance for the particles that rebound from the lateral surface of the plate. To do this, we introduce a fraction (phase) consisting of incident particles, i.e. particles flying to the surface of the body (plate), and another fraction (phase) consisting of reflected particles — particles flying away from the surface of the body counter to the incoming disperse flow. Collisions take place between these two particle phases. Since the collisions result in an exchange of momentum between particles in the different phases, the velocities of both the incident and the reflected particles also change. This in turn makes it necessary to introduce an effective force of interaction between the particles. Along with the momentum exchange, the collisions result in phase transformations in which incident particles are transformed into reflected particles and vice versa. Since the collisions take place in the presence of a third body, i.e. the dispersion medium, and since the friction of the gas causes the particles to be entrained toward the plate, the resulting phase transformation will be the transformation of reflected particles into incident particles. Thus, we introduce only one source term into the continuity equation for these phases. This term accounts for the transformation from reflected particles to incident particles. It should be noted that allowance for collisions between particles leads to randomization of their motion. Thus, additional terms will appear in the momentum and energy equations for the main body of particles and an additional particle phase located near the surface of the plate. The random motion of the latter phase is characterized by a certain internal energy, and the phase has a macroscopic velocity that is close to zero. Allowance for the above-mentioned

---

Moscow. Translated from Zhurnal Prikladnoi Mekhaniki i Tekhnicheskoi Fiziki, No. 6, pp. 67-74, November-December 1990. Original article submitted January 16, 1987; revision submitted October 22, 1987.

 0021-8944/90/3106-0860$12.50

terms and the additional phase appreciably complicates the system of equations: it now contains additional parameters whose values are not known beforehand. As a result of these complications, we will not take into account the randomization of the particles during the collisions. The equations which describe the given problem within the framework of a three-velocity, three-temperature scheme of motion have the following form [12]:

continuity equations for the gas and particles

$$\partial\rho_1/\partial t + \operatorname{div}(\rho_1\mathbf{v}_1) = 0,\ \partial\rho_i/\partial t + \operatorname{div}(\rho_i\mathbf{v}_i) = j_{ij} \tag{1.1}$$
$$(i,\ j = 2,\ 3;\ i \neq j);$$

equations of motion for the gas phase and disperse phase

$$\partial\rho_1\mathbf{v}_1/\partial t + \nabla^k\rho_1 v_1^k\mathbf{v}_1 + \nabla p = -\mathbf{f}_{12} - \mathbf{f}_{13},$$
$$\partial\rho_i\mathbf{v}_i/\partial t + \nabla^k\rho_i v_i^k\mathbf{v}_i = \mathbf{f}_{i1} - \mathbf{f}_{ij} + j_{ij}\mathbf{v}_3; \tag{1.2}$$

equations for the total energy of the mixture and the internal energy of the particles

$$(\partial/\partial t)\{\rho_1E_1 + \rho_2E_2 + \rho_3E_3\} + \operatorname{div}\{\rho_1E_1\mathbf{v}_1 +$$
$$+ \rho_2E_2\mathbf{v}_2 + \rho_3E_3\mathbf{v}_3\} + \operatorname{div}(p\mathbf{v}_1) = 0$$
$$\left(E_m = e_m + (1/2)\,\mathbf{v}_m^2,\quad m = 1,\ 2,\ 3\right), \tag{1.3}$$
$$\partial\rho_ie_i/\partial t + \nabla^k\rho_iv_i^ke_i = q_{1i} + j_{ij}e_3 + (1/2)\,\mathbf{f}_{ij}(\mathbf{v}_i - \mathbf{v}_j) + (1/2)\,j_{ij}(\mathbf{v}_i - \mathbf{v}_j)^2.$$

Here, the subscripts i, j = 2, 3; i ≠ j correspond to the parameters of the gas and the incident and reflected particles, respectively; the superscript k is the summation index and pertains to the coordinate axes; ρ_i, $\mathbf{v}_i$, e_i, E_i are the reduced density, velocity vector, and internal and external energies of the i-th phase; p is the pressure in the gas; $\mathbf{f}_{ij}$, q_{1i} are the friction vector and the rate of heat transfer between the gas and particles; $\mathbf{f}_{ij}$, j_{ij} are the vector of the effective force of interaction and the rate of mass transfer between the second and third phases as a result of the particle collisions. The last two terms in the equations for the internal energy of the incident (1 = 2) and reflected (j = 3) particles show that, due to force $(\mathbf{f}_{23}(\mathbf{v}_2 - \mathbf{v}_3))$ and mass $((1/2)j_{23}(\mathbf{v}_2 - \mathbf{v}_3)^2)$ intractions, the kinetic energy of the disperse particles that is dissipated in the form of heat is distributed equally between the phases of incident and reflected particles.

We will close system (1.1)-(1.3) with the equations of state of the phases

$$p = \rho_1^0(\gamma - 1)\,e_1,\ e_1 = c_{V1}T_1,\ e_2 = c_2T_2,\ e_3 = c_3T_3,\ \rho_2^0 = \rho_3^0 = \text{const}, \tag{1.4}$$

where γ is the adiabatic exponent of the gas; c_{V1}, $c_2 = c_3$ are the isochoric heat capacity of the gas and the heat capacity of the particles, respectively; T_i is the temperature of the phases; ρ_i^0 is the true density of the phase. We take the following equation to express the friction between the dispersion medium (gas) and the particles

$$\mathbf{f}_{1i} = (u_i/8)\,\pi dC_{di}\rho_1^0(\mathbf{v}_1 - \mathbf{v}_i)\,|\,\mathbf{v}_1 - \mathbf{v}_i\,|. \tag{1.5}$$

We use the following relations [13] for the drag coefficient of the particles:

$$C_{di}^0 = \frac{24}{\mathrm{Re}_{1i}} + \frac{4}{\sqrt{\mathrm{Re}_{1i}}} + 0.4,\quad C_{di} = C_{di}^0\,(1 + \exp(-0.423/\mathrm{M}_{1i})),$$
$$\mathrm{Re}_{1i} = \rho_1^0\,|\,\mathbf{v}_1 - \mathbf{v}_i\,|d/\mu_1 \tag{1.6}$$

(Re_{1i} is the Reynolds number of the particle flow; M_{1i} is the Mach number of this flow calculated from the local sonic velocity; n_i is the number of particles per unit volume).

We use the same expressions as in [14] for the effective force of interaction between the incident and reflected paticles $\mathbf{f}_{23}$ and the source term in the continuity equation which accounts for phase transformations of the type 3 → 2:

$$j_{23} = \frac{k^{(J)}\rho_2\rho_3 \,|\, \mathbf{v}_2 - \mathbf{v}_3 \,|}{\rho_2^0 d}, \quad \mathbf{f}_{23} = \frac{k^{(F)}\rho_2\rho_3 (\mathbf{v}_2 - \mathbf{v}_3) \,|\, \mathbf{v}_2 - \mathbf{v}_3 \,|}{\rho_2^0 d}$$

(d is the size of a particle). Here, the quantity $k^{(F)}$ determines the intensity of the mechanical interaction between the phases. In a study of the hydrodynamics of polydisperse flows in pipes [15], an expression was presented for the dependence of this coefficient on the difference in the velocities of the phases. For velocities ≈10 m/sec, $k^{(F)} \approx 0.1$. Extrapolating this relation to the case of velocities ≈100 m/sec, we can show that $k^{(F)} \approx 0.02$. The coefficient $k^{(J)}$, determining the rate of mass transfer, is of the same order as $k^{(F)}$ ($k^{(J)} = 0.08$). It should be noted that, as $k^{(F)}$, $k^{(J)}$ generally depends on the parameters of the dispersion medium and the disperse particles. Also, this relation may differ somewhat from the values of $k^{(J)}$ and $k^{(F)}$ used to perform the main calculations. The values of $k^{(F)}$ and $k^{(J)}$ can be refined further on the basis of an analysis of experimental data on the interaction of particles with one another in the flow of aerosols past solid bodies.

The following boundary conditions were assigned for system (1.1)-(1.6): a) on the left external boundary – the condition in the incoming flow; b) on the top and right external boundaries – the conditions of continuity of the flow, i.e., the derivatives of the flow parameters with respect to the normal to the theoretical region are equal to zero; c) in the plane of symmetry – the condition of symmetry of the flow; d) on the surface of the plate, the condition of nonflow for the gas and, for the particles, the condition of normal reflection with the coefficient $k^{(n)}$ $\left(v_3^x = -k^{(n)}v_2^x,\ v_3^y = v_2^y\right)$. The initial system of equations was changed to dimensionless form with respect to the parameters of the gas in the undisturbed flow and the linear dimension of the body. It can be shown that this system of equations and boundary conditions contains ten dimensionless determining parameters. The most characteristic of these parameters for the type of problems being examined here: the Mach number of the undisturbed flow M_∞; the adiabatic exponent of the gas γ; the reflection coefficient $k^{(n)}$; the mass concentration of particles in the undisturbed flow $r_{2\infty} = \rho_{2\infty}/\rho_{1\infty}^0$, where $\rho_{1\infty}^0$ is the true density of the gas in the undisturbed flow; the degree of inertia of the particles $\beta^{(v)} = 8\rho_2^0 d/(3\rho_{1\infty}^0 h)$ (h is the linear dimension); the parameter expressing the velocity disequilibrium of the incident and reflected particles $\beta_{32}^{(v)} = 3\beta^{(v)}/(8k^{(F)}r_{2\infty})$; the parameter characterizing the change in mass concentration due to collisions; $\beta_{32}^{(m)} = 3\beta^{(v)}/(8k^{(J)}r_{2\infty})$; the Reynolds number, calculated from the size of the particles: $\mathrm{Re}_d = \rho_{1\infty}^0 v_{1\infty}^x d/\mu_1$.

2. <u>Method of Numerical Integration</u>. We used the coarse-particle method [16, 17] to numerically integrate system (1.1)-(1.3). The scheme employed was of first-order accuracy. The accuracy of the results was checked by comparing numerical solutions obtained using different space and time steps in the integration. The difference between the results was no greater than 3-5% in any of the cases. In our investigation, we generalized the coarse-particle method to the case of a three-phase model of a gas with particles. As in the case of a two-phase model of motion, intermediate values are computed only for the gas phase at the Eulerian stage of the process. The parameters of the second and third phases remain constant during this stage, since there are no pressure gradients in the equations for the solid phase. In the Lagrangian stage, we calculate the transfer of the mass, momentum, and energy of each phase across the boundaries of the cells. In the final stage, we use the conservation laws to find the values of the parameters of all of the phase for the new time layer. Here, allowance is made for phase interaction f_{ij} ($i \neq j = 1, 2, 3$), the rate of mass transfer between the second and third phases j_{23}, and the heat fluxes q_{12}, q_{13} from the dispersion medium to the incident and reflected particles, respectively. As in the case of the two-dimensional model, the parameters of the solid phase are calculated first. The theoretical region we used was in the form of a rectangle divided into 42 cells lengthwise and 22 cells over its height. The value 0.082 was taken for the dimensionless spatial step in the integration $\Delta X = \Delta x/h$, while the time step ($\Delta\tau$) was found from the condition $\Delta\tau/\Delta x = 0.1$. Calculations were performed with different values of M_∞, $r_{2\infty}$, Re_d (Re_d is the Reynolds number calculated on the basis of the size of the particles), $k^{(J)}$, $k^{(F)}$, $k^{(n)}$, $\beta^{(v)}$ with fixed $\gamma = 1.4$, $c_{V1}/c_2 = 0.991$, $\mathrm{Pr} = 0.77$ (which corresponds, for example, to a mixture of air with solid particles).

3. <u>Description of the Results</u>. Figure 1 shows streamlines of the phases with $\beta^{(v)} = 4$, $k^{(J)} = 0.08$, $k^{(F)} = 0.02$, $k^{(n)} = 0.7$, $M_\infty = 3$, $r_{2\infty} = 1$, $\mathrm{Re}_d = 1287$. Here and below, unless otherwise noted the notation for the streamlines is as follows: gas phase – solid line; incident particles – dots; reflected particles – circles. Curves 1 and 2 show the wave (SW) in the gas and the envelope of streamlines of the reflected particles (separatrix). The calculations showed that, with

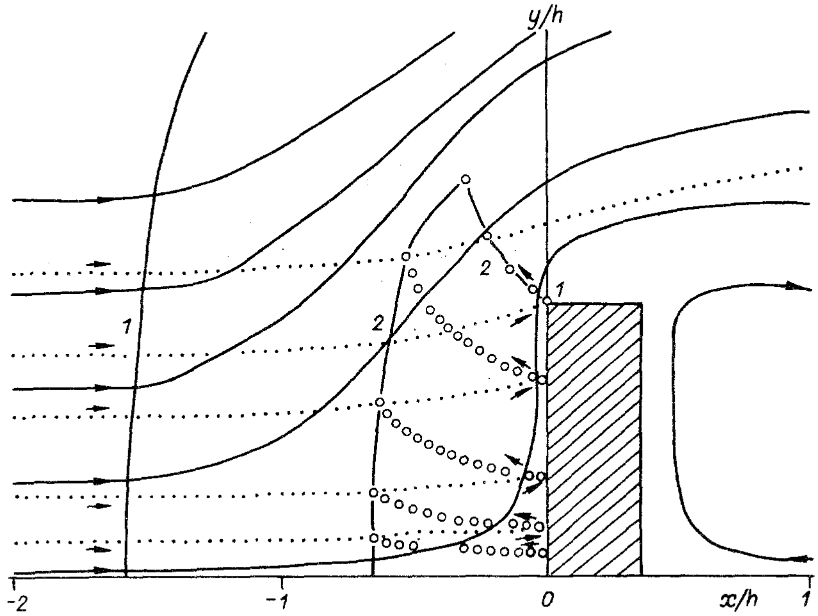

Fig. 1

allowance for reflected particles, the flow pattern in the case of supersonic flow past a bluff body can be described as follows. An outgoing shock wave is formed ahead of the body, and no disturbances from the body penetrate the incoming equilibrium flow behind this wave. Also located in front of the body is a zone of high particle concentration bounded by the separatrix. No reflected particles enter the incoming flow behind this zone, i.e., the separatrix is the envelope of the streamlines of the reflected particles. The normal velocity of these particles is equal to zero on the separatrix, and their concentration increases manyfold as they accumulate due to their slowing by the gas and the incident particles. The accumulation is limited by the transverse removal (blowing away) of particles by the gas moving toward the plate and by 3 → 2 phase transformations occurring due to collisions of the reflected particles with incident particles. As a result of these collisions, the reflected particles join the flow of incident particles.

The motion of the aerosol is characterized by the presence of two limiting cases. The first corresponds to the presence of very small particles, when the streamlines of the gas and particles nearly coincide. This case (conditionally designated as $\beta(v) = 0$ in the figures) was calculated on the basis of an equilibrium scheme for an effective gas with an altered sonic velocity in the gas phase and an altered adiabatic exponent. The calculations were performed by means of the standard equations of gas dynamics. The second limiting situation corresponds to the case of very large particles ($\beta^{(v)} = \infty$ in the figures), when the gas has no effect on particle motion and vice versa. The calculations for this case were performed in accordance with a frozen flow scheme in which the distributions of the parameters in the gas correspond to the absence of particles and the particles move along straight trajectories with an initial velocity. These calculations showed that the presence of reflected particles leads to a situation whereby no monotonic transition takes place from the case $\beta^{(v)} = 0$ to the case $\beta^{(b)} = \infty$, i.e., the distributions of the parameters in the gas are not found between the two limiting situations. Figures 2 and 3 show the distributions of the velocities of the phases and pressure in the gas along the plane of symmetry of the flow for different $\beta^{(v)}$ with the same $M_\infty, r_{2\infty}, k^{(F)}, k^{(J)}, k^{(n)}, \mathrm{Re}_d$, as in Fig. 1. Here and below, unless otherwise noted we used the following notation for the parameters: solid line) gas phase; dots) incident particles; circles) reflected particles; dot-dash line) case $\beta^{(v)} = \infty$; dot-dash line) $\beta^{(v)} = 0$. Curves 2-5 correspond to $\beta^{(v)} = 2.02$; 4.0; 40; 105.

The variants with increasing $\beta^{(v)}$ shown in Figs. 2 and 3 illustrate that the decay of the separatrix shock wave increase with an increase in $\beta^{(v)}$ from zero to a certain value $\beta^{(v)} \simeq 100$. Meanwhile, the decay of the wave in the gas is greater at $\beta^{(v)} = 4.05$ than at $\beta^{(v)} = \infty$. At values of $\beta^{(v)}$ exceeding 100, reflected particles fly out from behind the bow wave, creating a disturbance ahead of it and leading to the formation of two compression waves (see curves 4 in Figs. 2 and 3). In this case, the pressure on the body in general and

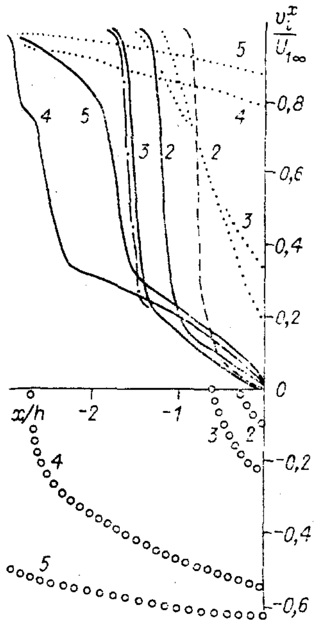

Fig. 2

at the stagnation point in particular (x = 0, y = 0) becomes less than the pressure for the regime of flow of a pure (without particles) gas ($\beta^{(v)} = \infty$) due to the additional curvature of the streamlines of the gas and its transverse removal. With a further increase in particle size, there is a tendency toward restoration of the bow wave and its return toward the body (see the curves in Figs. 2 and 3). This occurs as the flow pattern of the gas approaches that seen with the frozen flow scheme ($\beta^{(v)} = \infty$) corresponding to flow of the pure gas. In this range of regimes, with the movement of reflected particles out in front of the bow wave, events are dominated by the stagnting effect of the reflected particles on the gas rather than by the additional curvature of the gas streamlines. With a decrease in $\beta^{(v)}$, there is a more complete transfer of momentum from particles to gas. Thus, the pressure of the gas at the stagnation point also increases. It is found that the incident particles "press" the receding shock wave to the body, while the reflected particles "push it away" from the body. This pattern may introduce an element of nonmonoticity into the dependence of the distance between the shock wave and the body on the mass content of particles in the incoming flow.

Figure 4 shows distributions of the temperatures of the phases along the plane of symmetry for different $r_{2\infty}$ with the same $\beta^{(v)}$, $k^{(u)}$, $k^{(F)}$, $k^{(J)}$, M_∞, as in Fig. 1. Curves 1-4 correspond to $r_{2\infty} = 0$; 0.2; 0.5; 2. It is evident that decay of the shock wave increases somewhat with an increase in $r_{2\infty}$. A further increase in $r_{2\infty}$ leads to a reduction in this decay. This occurs because the attendant sharp increase in the number of collisions between reflected and incident particles results in a reduction in the size of the region occupied by reflected particles and produces a situation in which the effect of the incident particles on wave decay becomes stronger than the analogous effect of the reflected particles. It should also be noted that when the concentration of disperse phase in the incoming flow is high ($r_{2\infty} \risingdotseq 1$), the gas-temperature profile has a distinct nonmonotonic character (curve 4 in Fig. 4). This development is related to the occurrence of two competing processes in aerosols. The first is heat transfer between the gas and the particles, when heat is transferred from the highly heated gas to the colder particles. This leads to a decrease in the temperature of the gas in the shock layer. The second process is the dissipation of the kinetic energy of the particles into the heat energy of the gas due to the friction of the former against the gas. This process, conversely, leads to heating of the gas and an increase in its temperature in the shock layer. Immediately behind the shock wave, where the difference between the velocities of the gas and particles is large, the second process predominates over the first and the temperature of the gas increases; in the boundary region, where the velocities of the phases are low and the mass content of particles is high, the first process predominates and gas temperature decreases.

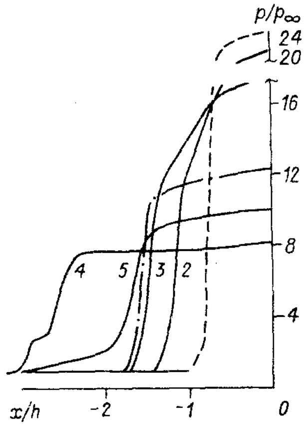

Fig. 3

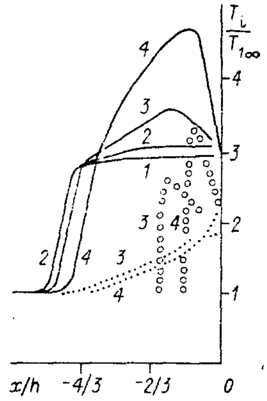

Fig. 4

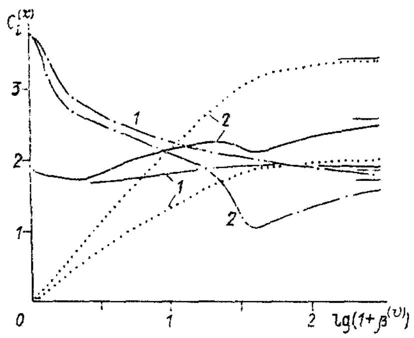

Fig. 5

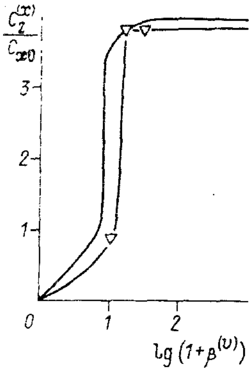

Fig. 6

Let us introduce a coefficient to account for the dynamic effect or wave resistance of the front surface of the body in a flowing aersol. This coefficient is equal to the ratio of the dynamic force F_1 acting along this surface to half the dynamic head of the gas in the incoming flow:

$$C_1^{(x)} = \frac{F_1}{(1/2)\,\rho_{1\infty}^0\left(v_{1\infty}^x\right)^2 h}, \quad F_1 = \int_0^h (p - p_\infty)\,dy$$

(the integral is taken over the front surface of the body in the flow). We also introduce coefficients to account for the dynamic effect of the particles $C_2^{(x)}$ and the drag of the plate $C^{(x)}$:

$$C_2^{(x)} = \frac{F_2}{(1/2)\,\rho_{2\infty}\left(v_{1\infty}^x\right)^2 h}, \quad F_2 = \int_0^h \left(1 + k^{(n)}\right)\rho_2\left(v_2^x\right)^2 dy,$$

$$C^{(x)} = \frac{F_1 + F_2}{(1/2)\left(\rho_{1\infty} + \rho_{2\infty}\right)\left(v_{1\infty}^x\right)^2 h} = \frac{\rho_{1\infty} C_1^{(x)} + \rho_{2\infty} C_2^{(x)}}{\rho_{1\infty} + \rho_{2\infty}}.$$

Figure 5 shows the dependence of the plate drag coefficient on $\beta^{(v)}$ at the same values of M_∞, $r_{2\infty}$, $k^{(F)}$, $k^{(J)}$, Re_d as in Fig. 1. The dot-dash lines correspond to $C_1^{(x)}$, the points to $C_2^{(x)}$, and the solid lines to $C^{(x)}$. Curves 1 correspond to $k^{(n)} = 0$, while curves 2 correspond to $k^{(n)} = 0.7$. Figure 5 shows that despite the marked dependence of $C_1^{(x)}$ and $C_2^{(x)}$ on $\beta^{(v)}$, at $k^{(n)} = 0$ the value of $C^{(x)}$ changes only slightly throughout the range of variation of $\beta^{(v)}$. At $k^{(n)} = 0.7$, there is a substantial change in $C^{(x)}$ at $\beta^{(v)} \geq 40$, when particles fly out in advance of the shock wave. In this case, the dependence of $C_1^{(x)}$ on $\beta^{(v)}$ is nonmonotonic. With an increase in $\beta^{(v)}$ from 0 to 40, the value of $C_1^{(x)}$ decreases because there is a decrease in the transfer of momentum from particles to gas. At $\beta^{(v)} \simeq 40$, there is a sharp reduction in $C_1^{(x)}$, since reflected particles fly out ahead of the shock wave into the incoming flow and the bow wave undergoes partial decay at these values of $\beta^{(v)}$. In this case, the effect of the dispersion medium is weaker due to the additional lateral movement of the gas caused by the screening effect of the reflected particles. With a further increase in $\beta^{(v)}$, the shock wave is restored and the coarse particles that fly out from behind it slow the gas only slightly. As a result, $C_1^{(x)}$ assumes a value close to that realized in the case of flow of the gas without particles. Thus, it can be concluded that in the cases trans- and supersonic flow past bluff bodies, the velocity disequilibrium of the phases which exists as the parameter $\beta^{(v)}$ changes from 1 to 100 has a substantial effect on the distribution of the parameters of the gas and particles in the shock layer. However, as is evident from Fig. 5, this disequilibrium — associated with the relative motion of the gas and the particles — has little effect on the force which is exerted by the two-phase flow on the plate and which can be characterized by the coefficient $C^{(x)}$ and the dynamic head $\rho_\infty(v_\infty^x)^2$. Thus, the equilibrium scheme for an effective gas can be used to calculate the total drag coefficient of the plate in the case of supersonic flow. For example, with $M_\infty = 3$, the difference between the maximum value of $C^{(x)}$ and the minimum value is 3% for the case when $k^{(n)} = 0$ (no reflected particles). If particles are present, the difference between the maximum $C^{(x)}$ and the minimum will be more substantial (about 20%). To check the adequacy of the proposed model in describing the physics of the problem in question, we compared numerical results with experimental data [4, 5]. Figure 6 shows the dependence of the corrected value of the coefficient expressing the dynamic effect of the particles on the plate $C_2^{(x)}/C_{x0}$ on the parameter $\beta^{(v)}$ (C_{x0} is the total drag coefficient of the plate at $r_{2\infty} = 0$) with $M_\infty = 0.6$ and $r_{2\infty} = 0.3$. The solid curve shows the calculated results, while the line with the triangles shows the experimental data [4]. The comparison with the data from [4, 5] shows that the difference is no greater than 10-15%, which confirms the reliability of the results obtained here.

LITERATURE CITED

1. A. P. Vasil'kov, "Neighborhood of the critical point of a bluff body in a hypersonic two-phase flow," Izv. Akad. Nauk SSSR Mekh. Zhidk. Gaza, No. 5 (1975).
2. Yu. P. Golovachev and A. A. Shmidt, "Supersonic flow of a dust-laden gas past a bluff body," ibid., No. 3 (1982).
3. Yu. M. Davydov and R. I. Nigmatulin, "Calculation of external heterogeneous flows of a gas with drops or particles past bluff bodies," Dokl. Akad. Nauk SSSR, 269, No. 1 (1981).
4. B. A. Balanin and V. A. Lashkov, "Resistance of a flat wedge in a two-phase flow," Izv. Akad. Nauk SSSR Mekh. Zhidk. Gaza, No. 2 (1982).
5. B. A. Balanin and V. V. Zlobin, "Experimental study of the aerodynamic resistance of simple bodies in a two-phase flow," Izv. Akad. Nauk SSSR Mekh. Zhidk. Gaza, No. 3 (1979).
6. N. N. Yanenko, A. P. Alkhimov, N. N. Nesterovich, et al., "Change in the wave structure in the movment of a supersonic two-phase flow past bodies," Dokl. Akad. Nauk SSSR, 260, No. 4 (1981).
7. N. N. Yanenko, R. I. Soloukhin, A. N. Papyrin, and V. M. Fomin, Supersonic Two-Phase Flows with Velocity Disequilibrium Between Particles [in Russian], Nauka, Novosibirsk (1980).
8. G. A. Saltanov, Nonequilibrium and Nonsteady Processes in the Gasdynamics of One- and Two-Phase Media [in Russian], Nauka, Moscow (1979).
9. G. A. Saltanov, Supersonic Two-Phase Flows [in Russian], Vyssh. Shkola, Minsk (1972).
10. S. K. Matveev, "Model of a gas of hard particles with allowance for inelastic collision," Izv. Akad. Nauk SSSR Mekh. Zhidk. Gaza, No. 6 (1983).
11. L. P. Seyukova, "Calculation of the flow of a dust-laden gas about a sphere with allowance for the effect of reflected particles," Gazodinamika Teploobmen, No. 7 (1982).
12. R. I. Nigmatulin, Principles of the Mechanics of Heterogeneous Media [in Russian], Nauka, Moscow (1978).
13. A. I. Ivandaev, A. G. Kutushev, and R. I. Nigmatulin, "Gasdynamics of multiphase media. Shock and detonation waves in aerosols," Itogi Nauki Tekh. Mekh. Zhidk. Gaza, 16, (1981).
14. I. Enikeev, "Effect of disperse particles reflected from the surface of a body in a flowing aerosol on the strucutre of the shock layer," in: Nonsteady Flows of Multiphase Systems with Physicochemical Transformations [in Russian], Izd. MGU, Moscow (1983).
15. T. L. Babukha and A. A. Shraiber, Interaction of Particles of a Polydisperse Material in Two-Phase Flows [in Russian], Naukova Dumka, Kiev (1972).

16. O. M. Belotserkovskii and Yu. M. Davydov, Coarse-Particle Method in Gasdynamics. Computational Experiment [in Russian], Nauka, Moscow (1982).
17. Yu. M. Davydov, "Coarse-particle method," in: Mathematical Encyclopedia, Vol. 3, Sov. Éntsiklopediya, Moscow (1982).